IEEE Photonics Journal
An IEEE Photonics Society Publication

Analysis of the Coupling Efficiency of a Dual-Fiber Spherical Coupler and Improvement of the Coupling Efficiency with a Polished Spherical Coupler

Volume 10, Number 4, August 2018

Yuanzheng Chen
Jiwen Cui
Jiubin Tan

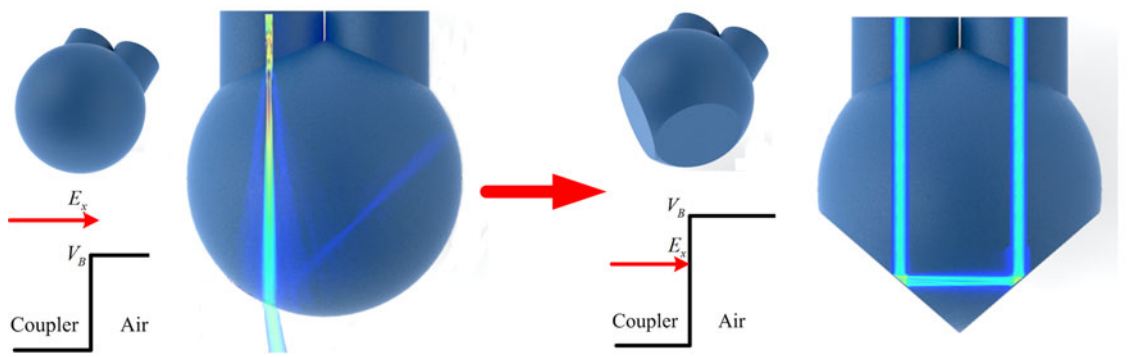

$V_B < E_x$ Coupling Efficiency is ~10%

$E_x < V_B$ Coupling Efficiency is improved to 22.9%

DOI: 10.1109/JPHOT.2018.2854837
1943-0655 © 2018 IEEE

Analysis of the Coupling Efficiency of a Dual-Fiber Spherical Coupler and Improvement of the Coupling Efficiency with a Polished Spherical Coupler

Yuanzheng Chen,[1,2] **Jiwen Cui**,[1,2] **and Jiubin Tan**[1]

[1]Center of Ultra-Precision Optoelectronic Engineering, Harbin Institute of Technology, Harbin 150001, China
[2]Yuanzheng Chen and Jiwen Cui contributed equally to this work

DOI:10.1109/JPHOT.2018.2854837

Manuscript received May 29, 2018; revised July 4, 2018; accepted July 6, 2018. Date of publication July 10, 2018; date of current version July 23, 2018. This work was supported in part by the National Natural Science Foundation of China (NSFC) under Grant 51575140 and in part by the Youth Talents Foundation of Harbin under Grant RC2016JQ006007. Corresponding author: Jiwen Cui (cuijiwen@hit.edu.cn).

Abstract: Efficient coupling of light from one waveguide to another is essential for many applications. The structural complexity of the coupler and the boundary discontinuity makes analyzing and improving the light energy coupling efficiency challenging. A dual-fiber spherical coupler, widely used in many fields, has a rather low coupling efficiency of 10%. The reasons for such low coupling efficiency have not yet been discussed, and effective methods for improving the coupling efficiency of this coupler have not been proposed. The coupling efficiency of the coupler is analyzed by using a proposed one-dimensional quantum tunneling model, and a polished spherical coupler is designed and fabricated to improve it. The main reason for the low coupling efficiency is that light has a rather high probability of refracting and then escaping at the boundary and that light reflects too many times inside the coupler. The polished coupler proposed effectively improved the coupling efficiency from 10% to 22.9%. This study will help researchers to design spherical couplers and promote their potential use.

Index Terms: Coupling efficiency, dual-fiber, spherical coupler.

1. Introduction

Efficient coupling of light from one waveguide to another is essential for many applications [1]–[3]. Analyzing and improving the light energy coupling efficiency (CE) is challenging because most waveguide couplers have a rather complex structure. A spherical light waveguide coupler is widely used in displacement sensors [4], [5], spherical coupling fiber probes for inner dimensional measurement [6], optical fiber couplings [7], fiber optic liquid level sensors [8], glucose sensors [9], resonant couplings [10], dual-fiber probes for depth-resolved fluorescence measurements [11], ball lens-based fiber probes in corneal and retinal imaging [12], etc. In these cases, the coupler has a complete or incomplete spherical waveguide, and the CE of light energy is quite low with an incomplete spherical coupler. Researchers have found that the CE of a typical dual-fiber spherical coupler (DSC), used to reverse the direction of input light, is only ∼10% [13]. The light energy loss in the optical fiber is rather low because of the total internal reflection caused by the special

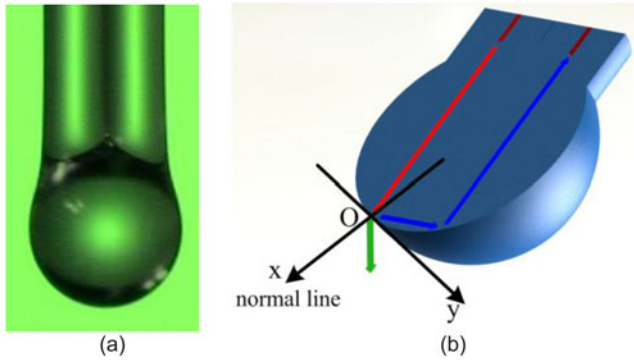

Fig. 1. (a) A Spherical coupler with a diameter of 330 μm under microscopy. The diameters of the input fiber and the output fiber are 125 μm. (b) Schematic of light transmission on the section plane. The axis *x* is along the direction of the normal line.

refractive index profile of the optical fiber, which indicates that most of the light energy is lost in the DSC. Optical fiber is difficult to use to obtain a stable returned light signal with such low CE caused by the high light energy loss.

Because the boundary of the dual-fiber spherical coupler is discontinues and the center of the sphere and the axis of the cylinder light waveguide are non-collinear, analyzing the light energy loss through it and proposing effective methods to improve CE have become challenging.

Cui experimentally studied the ratio of the diameter of a fiber to the diameter of a spherical coupler to improve the CE of the spherical coupler [14]. Eftimov used ray optics analysis to depict the redistribution of the input optical power and then experimentally tested the relationship between the form ratio and the back-coupled optical power [8]. Li proposed a Monte Carlo model to calculate the coupling efficiency of the coupler, and misalignment loss was investigated [15]. Sambanthan and Rahman presented a simple method based on chemical etching to improve the coupling efficiency between a laser diode and the coupler [16].

The analysis and experiments mentioned above are helpful to improve the CE of a DSC. However, there have been no reports discussing the reasons for the low coupling efficiency of the DSC, and effective methods for improving the CE have not yet been proposed.

In this study, a one-dimensional quantum tunneling model is proposed to analyze the reasons for the high loss of the light energy through the DSC. A polished DSC is proposed to improve the CE of the DSC, and the effectiveness of the proposed polished DSC is verified through simulations and experiments.

2. Analysis of the Light Energy Loss in the DSC

2.1 Effects of the Size of the DSC on the Incident Angle of Light at the Boundary of the Coupler

As shown in Fig. 1, a typical DSC is formed by fusing two cylindrical light waveguides such as optical fibers into one micro sphere. The size of the sphere is controllable by varying the current and the discharge time of the fiber fusion splicer. Light enters the spherical coupler through one optical fiber, reflects and refracts many times at the boundary of the spherical coupler, and finally enters the other optical fiber. The section plane *xOy* contains the principal axis of the input and output fibers. The returned light through the output fiber mainly consists of light transmitted in the planes parallel to the section plane. Light that is not parallel to the section plane *xOy* has a rather large probability of getting out of the spherical coupler rather than entering into the output fiber owing to the reflections and refractions. Therefore, the total light energy loss in the spherical coupler is mostly from the section plane.

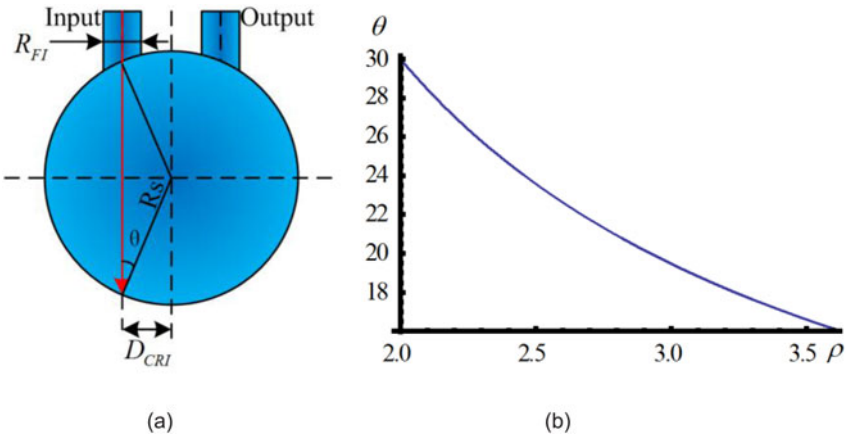

Fig. 2. Relationship between ρ and θ. D_{CRI} is the distance between the center of the sphere coupler and the axis of the input fiber, R_s is the radius of the sphere coupler, and R_{FI} is the radius of the input fiber. (a) Geometry analysis. (b) Calculated relationship between ρ and θ.

On the section plane, the incident light does not change direction until it travels to the boundary of the spherical coupler. The reflection and refraction at the boundary of the spherical coupler follow Snell's law. The refractive index of the spherical coupler is a constant in many studies, and the diameter of the spherical coupler affects the incident angle of the light. If we consider a more general situation, in which both the diameter of the spherical coupler and the two fibers are controllable, then the ratio ρ of the diameter of the spherical coupler to that of the two fibers affects the incident angle. The relationship between the ratio ρ and the incident angle θ is shown in Fig. 2(a).

The incident angle θ is expressed as

$$\theta = \arcsin \frac{D_{CRI}}{R_s} \tag{1}$$

When the interval between input and output fibers is negligible,

$$R_{FI} = D_{CRI} \tag{2}$$

If the diameters of the input fiber and the output fiber are equal, then

$$\rho = \frac{R_s}{R_{FI}} \tag{3}$$

For a typical DSC, the ratio ρ falls in the range of 2.0 to 3.2. The incident angle θ of the light at the boundary of spherical couplers with different ρ values is calculated, as shown in Fig. 2(b).

2.2 One-Dimensional Tunneling Model Used to Calculate the Probability of Reflection and Refraction at the Boundary of the DSC

As discussed above, in this study, the size of spherical coupler affects the incident angle of the light at the boundary. However, the relationship between the incident angle at the boundary of the spherical coupler and the probabilities of reflection and refraction have never been reported in the literature before, and the probabilities of refraction and reflection cannot be solved at a certain incident angle. Therefore, to calculate these probabilities, a one-dimensional tunneling model is proposed to depict the relationship between the probabilities of refraction and reflection at the boundary of the DSC and the incident angle, as shown in Fig. 3.

The reflection probability and the refraction probability are determined by the relationship between the potential energy V_B and E_x. The refractive index of the spherical coupler, n, is higher than that

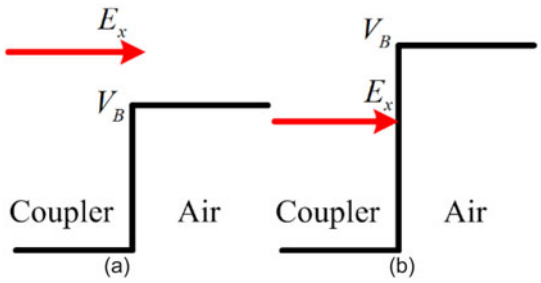

Fig. 3. One-dimensional quantum tunneling model used to calculate the probability of refraction and reflection at the boundary of the DSC. V_B is the potential height of the air along the x direction. E_x is the energy of the incident light along the x direction. (a) Situation when E_x is higher than V_B. (b) Situation when E_x is lower than V_B.

of air, and the function for one-dimensional quantum tunneling can be given by

$$V(x) = \begin{cases} 0, & x \leq 0 \\ V_B, & x > 0 \end{cases} \tag{4}$$

$$E_x = \langle x \mid \hat{E} \rangle \tag{5}$$

$$V_B = \hbar\upsilon \cos\left(\arcsin\frac{1}{n}\right) \tag{6}$$

According to the calculation, for a common DSC, E_x is much higher than V_B, as shown in Fig. 3(a). At the boundary of the DSC, the reflection probability P_R and the refraction probability P_T can be calculated using the following:When $V_B < E_x$, $x < 0$,

$$\nabla^2\varphi(x) + 2mE_x\varphi(x)/\hbar^2 = 0 \tag{7}$$

$$k = \sqrt{2mE_x}/\hbar \tag{8}$$

$$\varphi(x) = \exp(ikx) + R \times \exp(-ikx) \tag{9}$$

When $x > 0$,

$$\nabla^2\psi(x) + 2m(E_x - V_B)\psi(x)/\hbar^2 = 0 \tag{10}$$

$$k' = \sqrt{2m(E_x - V_B)}/\hbar \tag{11}$$

$$\psi(x) = T \times \exp(ik'x) \tag{12}$$

P_R and P_T can be calculated as

$$p_R = \left(\frac{k - k'}{k + k'}\right)^2 \tag{13}$$

$$p_T = \frac{4kk'}{(k + k')^2} \tag{14}$$

The above calculation shows that the probabilities of reflection and refraction are determined by E_x and V_B, where E_x is relative to the incident angle θ, and the potential energy V_B increases with the refractive index difference between the spherical coupler and air.

When E_x is higher than V_B, the probability of refraction, P_T, is much higher than that of reflection, P_R. Therefore, ~76% of the input light energy refracts at the boundary of the spherical coupler and escapes outside (Fig. 4(b)), and the remaining light in the DSC reflects many times with such a low reflection probability at the boundary before it travels to the output fiber. Most of the input light energy escapes outside and only ~10% finally exits the output fiber. As shown in Fig. 4(c),

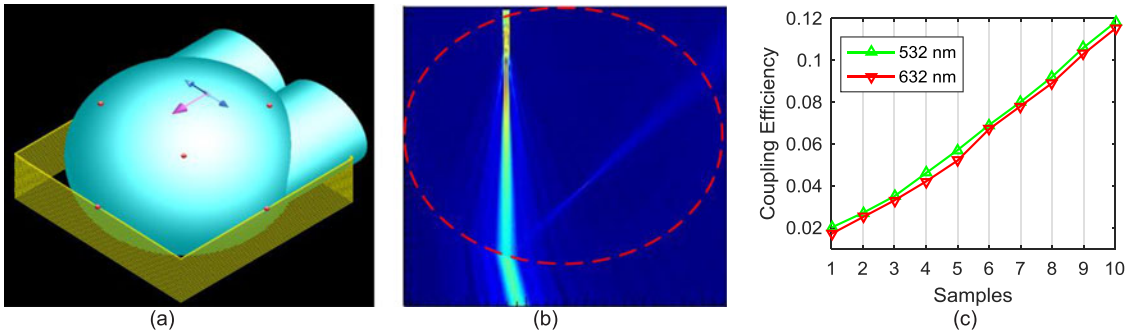

Fig. 4. Simulation of a DSC with a diameter of 330 μm by using the finite-difference time-domain method. (a) DSC model used for the simulation. (b) Light distribution on the *xOy* plane. The red line represents the boundary of the spherical coupler. (c) Simulation of DSCs with different ratios ρ.

TABLE 1
DSCs with Different Ratios ρ

Sample	Diameter of the sphere (μm)	Ratio ρ	Incident angle θ
1	399.6	3.2	18.2°
2	387.3	3.1	19.1°
3	375.4	3.0	19.8°
4	350.3	2.8	20.4°
5	337.8	2.7	21.7°
6	325.4	2.6	22.5°
7	312.9	2.5	23.4°
8	301.2	2.4	24.5°
9	274.8	2.2	26.4°
10	251.2	2.0	29.3°

simulations are run to investigate the CE of the DSCs listed in Table 1. When the wavelength of incident light is 532 nm, the CE is higher than that when the input wavelength is 632 nm. For a DSC with a constant angle θ, when the input wavelength increases, V_B decreases, and thus the difference between E_x and V_B increases. Therefore, the probability P_T increases when the incident wavelength increases; hence the CE drops as the incident wavelength increases.

Therefore, the main reason for the low CE for the DSC is the low reflection probability at the boundary of the sphere, and thus the light reflects too many times before exits the output fiber.

To improve the CE, a polished DSC is proposed to improve the reflection probability at the boundary of the sphere and reduce the number of times the light is reflected in the sphere simultaneously. As shown in Fig. 5(a), by polishing the sphere coupler, the incident angle of light at the boundary of the spherical coupler is reduced so as to ensure that $E_x < V_B$, thus ensuring that most of the light energy reflected into the spherical coupler. As shown in Fig. 5(c), compared to a normal DSC, the CE of the polished DSC improved dramatically from 10% to ~25%. Compared to the CE achieved with 532 nm input light, the CE is a little lower when the input light wavelength is 632 nm, and this trend is in accordance with the results shown in Fig. 4(c).

3. Experiments and Results

To verify the effect of the ratio ρ of the spherical coupler on the CE, an experiment was conducted with 10 DSCs with different ratios ρ, as given in Table 1.

The experimental setup is shown in Fig. 6(a). A diode pump solid state laser (DPSSL) with a wavelength of 532 nm and a He–Ne gas laser with a wavelength of 632 nm are used, and the power meters I and O used are PM100D models with a S120C probe from Thorlabs Company. Power meter I and power meter O simultaneously measure the light power of the input and output, respectively.

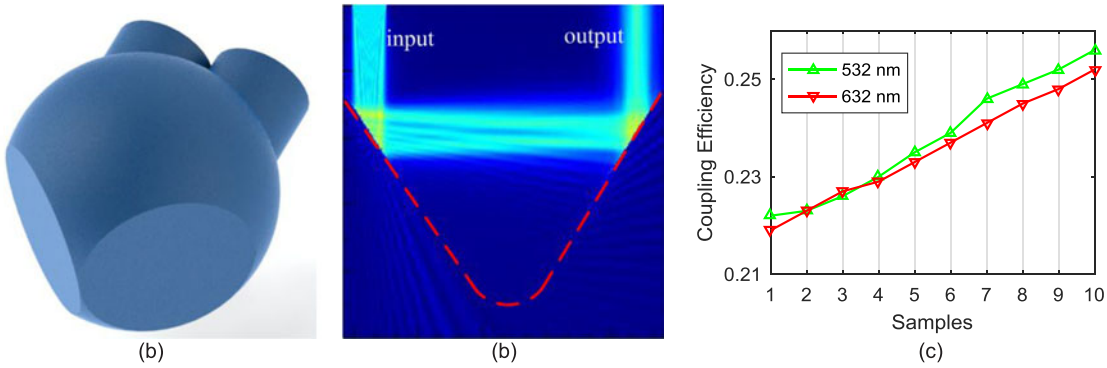

Fig. 5. Simulation of a polished DSC. (a) The interface of the spherical coupler is polished and formed a 45° plane. (b) Light energy distribution on the section plane *xOy*. The red line indicates the boundary of the polished DSC. (c) Simulation of polished DSCs with different ratios ρ.

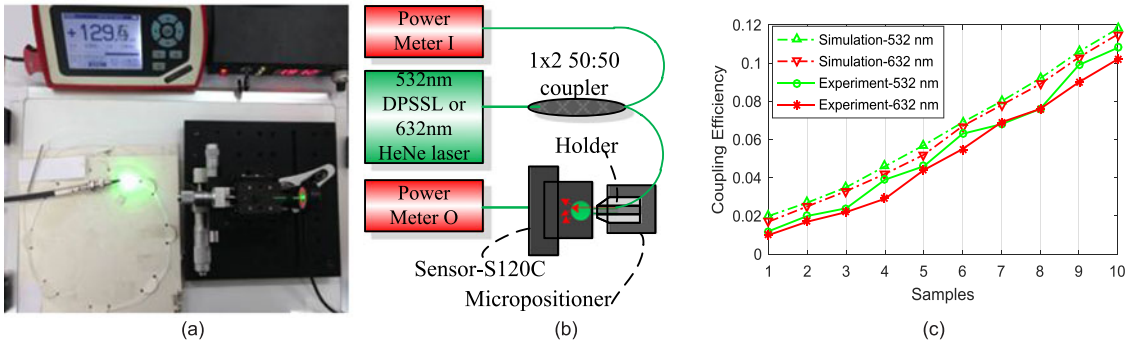

Fig. 6. Experiments of light energy loss in different spherical couplers. (a) Experimental setup. (b) Schematic of the experiment. The optical power meter measures the input and output light energy of the DSC. (c) Coupling efficiency of DSCs with different ratios ρ.

The optical fiber used in the experiment is SM450 from Thorlabs Company. To eliminate the random error measuring the diameter of the DSC samples, the average diameter from 10 measurements of a DSC sample is used as the diameter of the sample. Because the light through the DSC quickly decays in the output fiber, measuring the CE by plugging the output fiber end into the probe of the power meter sensor is inaccurate. In this experiment, the light energy escaping out of the DSC is measured, and the coupled light energy equals the input light energy minus the escaped light energy. Then, the CE of these DSCs is calculated, as shown in Fig. 6.

As shown in Fig. 6(c), simulations and experiments are in good accordance. When the incident angle increases from 18.2° to 29.3°, the CE of the DSCs gradually improves with both 532-and 632 nm input lights. With 532 nm input light, CE improves from 1.2% to 10.8%. With 632 nm input light, CE improves from 1% to 10.2%. Experimental results revealed that, when the incident angle increases from 18.2° to 29.3°, the difference between V_B and E_x decreases, and thus the probability P_R increases, thereby improving the CE of the DSC. However, E_x is still higher than V_B in this experiment, and the CE of the DSC could be further improved.

The DSCs listed in Table 1 are polished in our laboratory, and the CE of these DSCs is verified through experiments (Fig. 7). With 532 nm input light, the CE of these polished DSCs falls in the range of 19.8% to 22.9%, and the difference between the maximum and minimum CE values is only 3.1%. With 632 nm input light, the CE of these polished DSCs falls in the range of 19.3% to 22.6%. Simulation and experimental results are in good accordance. The CE achieved from experiments is a little lower than that achieved from simulations, which is caused by the incomplete nature of

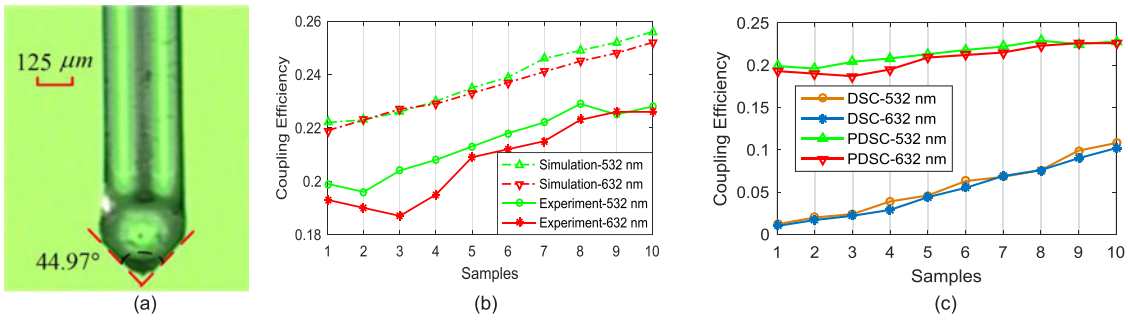

Fig. 7. Experiment polished DSCs. (a) Polished DSC. (b) The CE of polished DSCs. (c) Experimental test of CE of DSCs before and after polishing.

the sphere. These experimental results indicate that, when the number of times light reflects in the DSC and the probability P_T are both constants, the ratio ρ has little effect on the CE of the DSC. It is therefore concluded that the number of times light reflects in the sphere (TLR) and the probability P_T determine the CE and that the CE of a DSC is inversely proportional to both TLR and P_T. By polishing the DSC, both the probability P_T and TLR are decreased simultaneously, dramatically improving the CE from ∼10% to 22.9%.

4. Conclusion

This study provides an explanation for the low CE of a DSC from the point of view of the probabilities of the refraction and reflection of light at the boundary of the spherical coupler by using the proposed one-dimensional quantum tunneling model. The main reason for the low CE of a DSC is that light has a rather higher probability of refracting at the boundary of the DSC than reflecting and that the light reflects too many times in the DSC.

When the ratio ρ is decreased from 3.2 to 2.0, the CE of the DSC is improved from 1.2% to 10.8%, and this is caused by the decrease of the difference between V_B and E_x, increasing the probability P_R. The CE of an unpolished DSC decreased when the wavelength of the input light increased, because of the increase in the difference between E_x and V_B increased P_T.

The polished DSC proposed in this study effectively reduced the probability P_T and TLR simultaneously, and the CE of the DSC dramatically improved from 10.8% to 22.9% with 532 nm input light and from 10.2% to 22.6% with 632 nm input light.

The conclusions discussed above are verified through experiments and simulations. Experimental results are in a good accordance with simulation results.

This study proposes a new method for calculating the CE between two waveguides and proposes an effective method to improve the CE of a DSC dramatically. It will help researchers to design spherical couplers and promote their potential use.

References

[1] X. Zhou, Z. Chen, Z. Wang, and J. Hou, "Monolithic fiber end cap collimator for high-power free-space fiber-fiber coupling," *Appl. Opt.*, vol. 55, no. 15, pp. 4001–4004, 2016.
[2] X. Zhao, H. Dalir, X. Xu, and R. T. Chen, "Efficient coupling into slow-light one-dimensional fishbone waveguide by mode converter method," *Appl. Phys. Exp.*, vol. 10, no. 7, Art no. 072502, 2017.
[3] L. Yang, D. Dai, B. Yang, Z. Sheng, and S. He, "Characteristic analysis of tapered lens fibers for light focusing and butt-coupling to a silicon rib waveguide," *Appl. Opt.*, vol. 48, no. 4, pp. 672–678, 2009.
[4] A. A. Jasim, A. Z. Zulkifli, M. Z. Muhammad, S. W. Harun, and H. Ahmad, "A new compact micro-ball lens structure at the cleaved tip of microfiber coupler for displacement sensing," *Sens. Actuators, A*, vol. 189, no. 2, pp. 177–181, 2013.
[5] B. Guzowski, M. Lakomski, and M. Cywinsk, "Proximity sensors based on ball-lensed optical fibers," *IOP Conf. Ser.: Mater. Sci. Eng.*, vol. 104, no. 1, Art no. 012031, 2015.

[6] J. Cui, Y. Chen, and J. Tan, "Improvement of dimensional measurement accuracy of microstructures with high aspect ratio with a spherical coupling fiber probe," *Meas. Sci. Technol.*, vol. 25, no. 7, Art no. 075902, 2014.
[7] S. D. Alaruri, "Single-mode fiber-to-single-mode fiber coupling efficiency and tolerance analysis: Comparative study for ball, conic and GRIN rod lens coupling schemes using Zemax Huygen's integration and physical optics calculations," *Optik*, vol. 126, no. 24, pp. 5923–5927, 2015.
[8] T. A. Eftimov and W. J. Bock, "A simple multifunctional fiber optic level/moisture/vapor sensor using large-core quartz polymer fiber pairs," *IEEE Trans. Instrum. Meas.*, vol. 55, no. 6, pp. 2080–2087, Dec. 2006.
[9] S. W. Harun, A. A. Jasim, H. A. Rahman, M. Z. Muhammad, and H. Ahmad, "Micro-ball lensed fiber-based glucose sensor," *IEEE Sens. J.*, vol. 13, no. 1, pp. 348–350, Jan. 2013.
[10] O. V. Svitelskiy, Y. Li, M. Sumetsky, D. Carnegie, E. Rafailov, and V. N. Astratov, "Resonant coupling to microspheres and light pressure effects in microfluidic fiber-integrated platforms," in *Proc. IEEE Photonic Soc. 24th Annu. Meeting*, vol. 58, no. 11, 2011, pp. 185–186.
[11] H. Y. Choi *et al.*, "Microlensed dual-fiber probe for depth-resolved fluorescence measurements," *Opt. Exp.*, vol. 19, no. 15, pp. 14172–14181, 2011.
[12] M. Zhao, Y. Huang, and J. U. Kang, "Sapphire ball lens-based fiber probe for common-path optical coherence tomography and its applications in corneal and retinal imaging," *Opt. Lett.*, vol. 37, no. 23, pp. 4835–4837, 2012.
[13] J. Cui, L. Li, and J. Tan, "Optical fiber probe based on spherical coupling of light energy for inner-dimension measurement of microstructures with high aspect ratios," *Opt. Lett.*, vol. 36, no. 23, pp. 4689–4691, 2011.
[14] J. Cui, L. Li, and J. Tan, "Opto-tactile probe based on spherical coupling for inner dimension measurement," *Meas. Sci. Technol.*, vol. 23, no. 23, pp. 85105–85115, 2012.
[15] S. Li, Y. Sun, J. Zhu, and T. Tang, "Monte Carlo simulation for coupling between single-mode fiber and slab waveguide with spherical fiber microlenses," *Opt. Eng.*, vol. 50, no. 11, Art no. 115001, Nov. 2011.
[16] K. Sambanthan and F. A. Rahman, "Method to improve the coupling efficiency of a hemispherically lensed asymmetric tapered-core fiber," *Opt. Commun.*, vol. 254, no. 1–3, pp. 112–118, 2005.